Impairment in Sulfite Reductase Leads to Early Leaf Senescence in Tomato Plants[1][W][OPEN]

Dmitry Yarmolinsky, Galina Brychkova, Assylay Kurmanbayeva, Aizat Bekturova, Yvonne Ventura, Inna Khozin-Goldberg, Amir Eppel, Robert Fluhr, and Moshe Sagi*

The Jacob Blaustein Institute for Desert Research, Albert Katz Department of Dryland Biotechnologies, Ben-Gurion University of the Negev, Beer Sheva 84105, Israel (D.Y., G.B., A.K., A.B., Y.V., I.K.-G., A.E., M.S.); and Department of Plant Sciences, Weizmann Institute of Science, Rehovot 76100, Israel (R.F.)

Sulfite reductase (SiR) is an essential enzyme of the sulfate assimilation reductive pathway, which catalyzes the reduction of sulfite to sulfide. Here, we show that tomato (*Solanum lycopersicum*) plants with impaired SiR expression due to RNA interference (SIR Ri) developed early leaf senescence. The visual chlorophyll degradation in leaves of SIR Ri mutants was accompanied by a reduction of maximal quantum yield, as well as accumulation of hydrogen peroxide and malondialdehyde, a product of lipid peroxidation. Interestingly, messenger RNA transcripts and proteins involved in chlorophyll breakdown in the chloroplasts were found to be enhanced in the mutants, while transcripts and their plastidic proteins, functioning in photosystem II, were reduced in these mutants compared with wild-type leaves. As a consequence of SiR impairment, the levels of sulfite, sulfate, and thiosulfate were higher and glutathione levels were lower compared with the wild type. Unexpectedly, in a futile attempt to compensate for the low glutathione, the activity of adenosine-5′-phosphosulfate reductase was enhanced, leading to further sulfite accumulation in SIR Ri plants. Increased sulfite oxidation to sulfate and incorporation of sulfite into sulfoquinovosyl diacylglycerols were not sufficient to maintain low basal sulfite levels, resulting in accumulative leaf damage in mutant leaves. Our results indicate that, in addition to its biosynthetic role, SiR plays an important role in prevention of premature senescence. The higher sulfite is likely the main reason for the initiation of chlorophyll degradation, while the lower glutathione as well as the higher hydrogen peroxide and malondialdehyde additionally contribute to premature senescence in mutant leaves.

Sulfur is a constituent of many important biological compounds including amino acids, the redox-buffering tripeptide glutathione, polysaccharides, coenzymes, sulfolipids, and many secondary metabolites (Amtmann and Armengaud, 2009). Plants are able to reduce inorganic sulfate to sulfide, which is subsequently incorporated into organic molecules. This process consists of successive enzymatic reactions that occur in chloroplasts of plant cells. Sulfate is transported to chloroplasts (Cao et al., 2013), where it is adenylated by ATP:sulfate adenylyltransferase (ATPS; EC 2.7.7.4). The product of this reaction, adenosine-5′-phosphosulfate (APS), is reduced with the formation of toxic sulfite by APS reductases (APRs; EC 1.8.4.9) employing reduced glutathione (GSH). The further reductive assimilation of sulfite is catalyzed by sulfite reductase (SiR; EC 1.8.7.1) that contains one iron-sulfur cluster and one siroheme as prosthetic groups and uses reduced ferredoxin as the physiological donor of the six-electron reduction of sulfite to sulfide (Nakayama et al., 2000; Yonekura-Sakakibara et al., 2000). The latter is incorporated by *O*-acetyl-Ser (thiol) lyases (EC 2.5.1.47) into Cys that can be used for glutathione synthesis (Yi et al., 2010; Takahashi et al., 2011).

In addition to reductive assimilation, plants can perform alternative sulfite conversion. The oxidation of sulfite to sulfate is catalyzed by sulfite oxidase (SO; EC 1.8.3.1) and is considered as the main avenue in plant protection against sulfite toxicity (Brychkova et al., 2007; Lang et al., 2007). Sulfur transferases (STs; EC 2.8.1.2) also participate in sulfite detoxification by the synthesis of the less toxic thiosulfate from β-mercaptopyruvate and sulfite (Papenbrock and Schmidt, 2000; Tsakraklides et al., 2002). UDP-sulfoquinovose synthase1 (SQD1; EC 3.13.1.1) utilizes sulfite for the biosynthesis of sulfoquinovosyl diacylglycerols (SQDGs; sulfolipids) required for proper function of the photosynthetic membranes (Sanda et al., 2001). The molecular factors and enzymes were shown recently to act as a network in maintaining sulfite homeostasis in plants (Tsakraklides et al., 2002; Brychkova et al., 2013).

As with other nutrient metabolic pathways in plants, the enzymes required for sulfur assimilation and thiol metabolism are highly regulated and tightly coordinated at many levels (Yi et al., 2010). The flux of metabolites via the sulfate assimilation reductive pathway is controlled by APR enzymes whose expression is modulated by sulfate as well as nitrate availability and various stress factors (Leustek et al., 2000; Martin et al., 2005). However, it was recently revealed that SiR plays a more

[1] This work was supported by the Chief Scientist, Ministry of Agriculture and Rural Development, Israel (grant no. 857–0549–08) and by the Israel Science Foundation (grant no. 212/13).

* Address correspondence to gizi@bgu.ac.il.

The author responsible for distribution of materials integral to the findings presented in this article in accordance with the policy described in the Instructions for Authors (www.plantphysiol.org) is: Moshe Sagi (gizi@bgu.ac.il).

[W] The online version of this article contains Web-only data.

[OPEN] Articles can be viewed online without a subscription.

www.plantphysiol.org/cgi/doi/10.1104/pp.114.241356

important role in the regulation of sulfate assimilation than previously supposed. Arabidopsis (*Arabidopsis thaliana*) plants with lowered SiR activity exhibited dramatically reduced biomass production as well as marked disturbances in plant metabolism, indicating that SiR is essential for plant growth and plays a flux-controlling role in the sulfate assimilation reductive pathway (Khan et al., 2010).

Although SiR exhibits a semiconstitutive pattern of expression (Khan et al., 2010), this enzyme was induced by short-term sulfite application (Brychkova et al., 2007, 2013; Yarmolinsky et al., 2013) as well as long-term SO_2 fumigation (Randewig et al., 2012). By employing tomato (*Solanum lycopersicum*) and Arabidopsis SiR mutants overexpressing or impaired in SiR activity, it was recently demonstrated that SiR not only functions as a component of the sulfate assimilation reductive pathway but also plays a role in protecting plants against sulfite toxicity (Yarmolinsky et al., 2013). Importantly, the plastidic 70-kD SiR enzyme acts as a binding protein in the plastidic DNA organization in addition to its functions in sulfite conversion (Cannon et al., 1999; Sato et al., 2001; Chi-Ham et al., 2002; Sekine et al., 2002, 2007; Kang et al., 2010).

Here, we show that impairment in tomato SiR expression resulted in accelerated yellowing of the cotyledons and later in the lower leaves of older plants, while the upper leaves remained unaffected. In this study, we demonstrated that the restriction of sulfate reduction due to SiR impairment leads to a deregulation of the sulfate assimilation reductive pathway, resulting in decreased glutathione in SiR-impaired plants. The consequent enhancement of sulfate assimilation pathways causes further sulfite overproduction and results in senescence-like damage of tomato leaves.

RESULTS

SiR-Impaired Plants Demonstrate Early Leaf Senescence

Suppression by RNA interference was recently shown to down-regulate SiR transcript, protein, and activity (Yarmolinsky et al., 2013). Independent lines with impaired SiR expression due to RNA interference (SIR Ri), SIR Ri37, and SIR Ri40, displayed phenotypes of yellow spots on the older leaves and were employed in this study to unravel the connection between SiR impairment and accelerated chlorophyll degradation.

The first clear-cut abnormality that distinguished SIR Ri plants from the wild-type plants was early necrosis and chlorophyll degradation in cotyledons at the age of 2 to 3 weeks (Fig. 1A). We further compared SIR Ri with wild-type leaves at different stages of development. For 1-month-old plants, the following wild-type leaves were compared with the corresponding SIR Ri leaves: (1) the first and second leaves as counted from the top, (2) the third leaf from the top, and (3) the fifth leaf from the top. For the 2- or 3-month-old plants, we compared the third, fifth, and seventh or third and sixth wild-type leaves, respectively, with the corresponding leaves of SIR Ri plants. The SIR Ri plants were characterized by obvious fast yellowing of the older (lower) leaves, while the corresponding leaves of the wild-type plants remained green or demonstrated only slight change in color. This phenotype was observed throughout the life span of SIR Ri plants (Fig. 1B; Supplemental Fig. S1). In general, the SIR Ri37 line demonstrated more pronounced symptoms of early leaf senescence than SIR Ri40 plants (Fig. 1; Supplemental Fig. S1), probably due to multiple insertions in its genome (Yarmolinsky et al., 2013).

In addition to the decreased chlorophyll content (Fig. 1; Supplemental Fig. S1), the photosynthetic efficiency in the yellowing leaves of SIR Ri plants was reduced. The maximum photochemical efficiency of PSII in the dark-adapted state (F_v/F_m) was substantially decreased in the lower leaves of SIR Ri plants compared with the upper leaves of the same plants as well as with the corresponding lower leaves of the wild type (Fig. 1C; Supplemental Fig. S1). Imaging of PSII activity in the whole tomato leaves revealed its uneven distribution in the lower leaves of SIR Ri plants, where the F_v/F_m ratio was greatly reduced at the edges, while the tissue in the vicinity of the large vessels remained mostly unaffected (Supplemental Fig. S2).

Enhanced production of reactive oxygen species (ROS) as well as malondialdehyde (MDA), a marker for lipid peroxidation, is characteristic of naturally senescent leaves (Dhindsa et al., 1981; Khanna-Chopra, 2012; Wang et al., 2013). Staining leaves with 3,3′-diaminobenzidine (DAB) revealed significantly higher levels of hydrogen peroxide in the third and the fifth leaves of 1-month-old SIR Ri plants compared with the wild type (Supplemental Fig. S3). Importantly, MDA level increased with the age of SIR Ri leaves and, unlike the generation of ROS, was higher in all the tested leaves of SIR Ri plants compared with the wild type (Supplemental Fig. S3). These results indicate that MDA and ROS are indicative, if not the cause, of the decrease in quantum yield and chlorophyll content in the leaves of SIR Ri plants.

The casein lytic proteinase (Clp) complex is the most abundant protease in the chloroplast stroma and is known to be involved in controlling leaf senescence and response to various stress factors (Roberts et al., 2012). An ATP-dependent Clp protease regulatory subunit clpD (encoded by *senescence associated gene15*) was associated with leaf senescence in aspen (*Populus tremula*) and Arabidopsis plants (Roberts et al., 2012). Significant up-regulation of *clpD* transcript was evident in the lower leaves of SIR Ri plants (Fig. 1D; Supplemental Fig. S1A), indicating an enhanced degradation of chloroplast proteins as a result of SiR impairment. The levels of autophagy-related protein8a (ATG8a) were also higher in SIR Ri plants than in the wild type plants, reflecting enhanced autophagy processes (Fig. 2B). Taking together the enhanced degradation of chlorophyll, the reduction of maximal quantum yield, the enhanced catabolic processes, and the increase in MDA and ROS concentrations, our results clearly indicate that SiR impairment results in early leaf senescence phenotype in tomato plants.

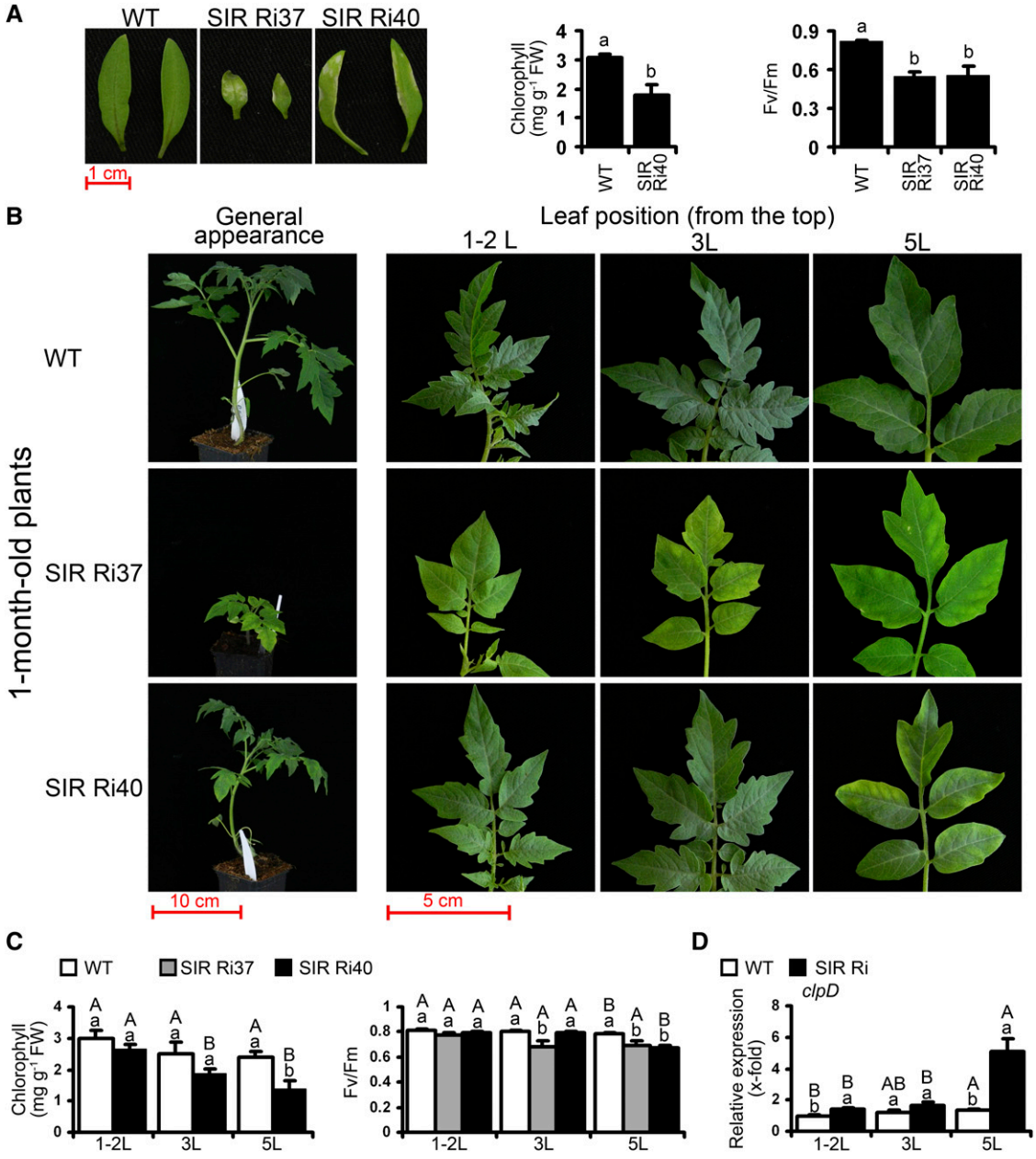

Figure 1. Early leaf senescence in SiR-impaired tomato plants compared with the wild type (WT). A, The damage on cotyledons of SIR Ri plants at the age of 2 weeks (left). Chlorophyll content and F_v/F_m in the cotyledons of SIR Ri lines are shown in the middle and right, respectively. The bars represent the average ± SE ($n = 6$ in the chlorophyll assay; $n = 8$ for the wild type and SIR Ri37; and $n = 5$ for SIR Ri40 in the F_v/F_m assay). B, Leaf phenotypes of wild-type and SIR Ri plants at the age of 1 month. The top (1-2L), the third (3L), and the fifth (5L) leaves counted from the tops are shown together with the general plant appearance. C, Chlorophyll content (left) and maximal quantum yield (middle) in the 1-month-old tomato plants. Bars represent the average values ± SE ($n = 5$ in the chlorophyll assay; $n = 4$ for the wild type; $n = 6$ for Ri37; and $n = 4$ for SIR Ri40 in the F_v/F_m assay). D, Expression of *clpD* transcript in the 1-month-old tomato plants. The values are average ± SE ($n = 8$ for the wild type and SIR Ri [average of SIR Ri37 and SIR Ri40 plants]). Transcript quantification was performed by real-time PCR using *TFIID* (*SGN-U571616*) as a housekeeping gene. The values were normalized to the top leaf of the wild type. The values denoted with different letters are significantly different according to the Tukey-Kramer honestly significant difference mean-separation test (JMP 8.0; $P < 0.05$). The uppercase letters reflect differences between leaves of the same genotype; the lowercase letters distinguish different genotypes. The scale bars are shown.

Molecular Components Associated with Chlorophyll Breakdown Lead to Early Chlorophyll Degradation in Leaves of SiR-Impaired Plants

Chlorophyll breakdown is an obvious feature of leaf senescence and is catalyzed by a number of enzymes whose expression is tightly regulated to avoid accumulation of highly toxic intermediate products (Hörtensteiner and Kräutler, 2011). The accelerated degradation of chlorophyll in SIR Ri plants led us to investigate the mechanism/s of chlorophyll catabolism in the 1- and 2-month-old plants (Fig. 2A; Supplemental Fig. S4A). Importantly, the transcript encoding STAY-GREEN1 (SGR1) protein, the initiator of chlorophyll breakdown in chloroplasts (Sakuraba et al., 2012), was significantly enhanced in the lower leaves of SIR Ri plants compared with both the young leaves of the same plants and with the leaves of wild type plants (Fig. 2A; Supplemental Fig. S4A). Similar to *SGR1*, the transcript of *PHEOPHYTINASE* (*PPH*) gene, which encodes the protein involved in the first step of chlorophyll breakdown (Hörtensteiner and Kräutler, 2011), was clearly up-regulated in SIR Ri plants (Fig. 2A; Supplemental Fig. S4A). PHEIDE A OXYGENASE (PAO) catalyzes the key reaction of chlorophyll catabolism, porphyrin macrocycle cleavage of pheophorbide A to a primary fluorescent catabolite (Pruzinská et al., 2003; Hörtensteiner and Kräutler, 2011). Although there were no differences in *PAO* transcript levels between the genotypes, western immunoblotting analysis revealed that the lower leaves of both wild-type and SIR Ri plants expressed high levels of PAO protein (Fig. 2B). However, a significantly higher level of PAO protein was found in the fifth leaves of SIR Ri40 plants compared with the corresponding leaves of the wild-type plants. The difference between PAO transcript and PAO protein likely reflects existence of posttranscriptional mechanisms regulating PAO expression. Importantly, unlike the 1-month-old plants, both the PAO protein and transcript in the lower leaves of the 2-month-old plants were clearly enhanced in SIR Ri plants compared with the wild type (Supplemental Fig. S4B). The increase in expression of PAO in SIR Ri plants indicates that SiR impairment likely leads to chlorophyll degradation by the PAO pathway shown to be activated during natural leaf senescence (Hörtensteiner and Kräutler, 2011).

Altered Expression of Photosynthesis-Related Plastidic Proteins in SIR Ri Leads to the Reduction in PSII Activity

The decrease in maximal quantum yield, which was observed in leaves of SIR Ri plants, could be associated with reduced levels of plastidic proteins functioning in the photosystem. D1 protein (encoded by *psbA* transcript), a component of the reaction center of PSII (Keren et al., 1997), and psbO, one of the subunits that construct the water-splitting system of PSII (Roose et al., 2010), were significantly lower in SIR Ri than in the 1-month-old (Fig. 2B) and 2-month-old wild-type leaves (Supplemental Fig. S4B). While the wild-type plants demonstrated an enhancement of D1 and psbO proteins in their lower leaves compared with the young top leaves, the mutants showed only a slight enhancement or a decrease in the levels of these proteins in the lower leaves. The 2-month-old SIR Ri plants additionally showed a significant reduction of light-harvesting chlorophyll *a*/*b*-binding protein1 (Lhcb1) and ferredoxin1 (Fdx1; Supplemental Fig. S4B). Similarly, levels of the large subunits of Rubisco (LSU/Rubisco) and small subunits of Rubisco (SSU/Rubisco) were significantly lower in the lower leaves of SIR Ri plants compared with the leaves at the same position in wild-type plants (Fig. 2B; Supplemental Fig. S4B).

We also quantified the relative expression of chloroplastic genes encoding selected proteins of the PSII core complex (psbA, psbB, psbC, and psbD) as well as LSU/Rubisco and clpP1. The latter is a central component of the Clp chloroplastic proteolytic complex and is encoded by the chloroplast genome, while all the other Clp components are nucleus-encoded proteins (Sokolenko et al., 2002; Peltier et al., 2004). The young top leaves of the 1-month-old SIR Ri plants exhibited a slight reduction of *psbA*, *LSU/Rubisco*, and *clpP1* transcripts (approximately 80% of the wild-type level), while the other genes remained unaffected (Fig. 2C). Significantly, a more pronounced reduction was shown in the expression of *psbA*, *psbB*, *psbC*, *psbD*, and *LSU/Rubisco* and *clpP1* transcripts in the third and/or fifth and/or seventh leaves (from the top) of SIR Ri plants compared with the wild type (Fig. 2C; Supplemental Fig. S4C). The suppressed expression of the *psbA* transcript encoding the D1 protein was in agreement with the reduced levels of this protein in the leaves of SIR Ri plants (Fig. 2, B and C; Supplemental Fig. S4, B and C).

The Impact of SiR Impairment on Sulfur Metabolism in Tomato Plants

One can expect that damage to the chloroplast in SIR Ri plants would be associated with a disturbance in sulfur metabolism that occurred in SiR-impaired plants (Khan et al., 2010; Yarmolinsky et al., 2013). To address this question, we measured major sulfur metabolites in SIR Ri and wild-type tomato plants.

Concentrations of sulfite and total glutathione were the highest in the top unextended leaves, decreasing with leaf age. By contrast, sulfate and thiosulfate were associated with leaf age, being higher in the lower leaves compared with the younger upper leaves (Fig. 3; Supplemental Fig. S5). Sulfur metabolism in SIR Ri tomato plants significantly differed from that of wild-type plants. Glutathione levels were decreased in all the leaves of the 2-week-old SIR Ri seedlings, including cotyledons, while the same leaves demonstrated considerably increased sulfite compared with the wild type (Fig. 3A). Older SIR Ri plants at the age of 1 and 2 months also exhibited a decrease in glutathione levels in all of their leaves compared with the wild-type leaves (Fig. 3B; Supplemental Fig. S5). As opposed to levels of

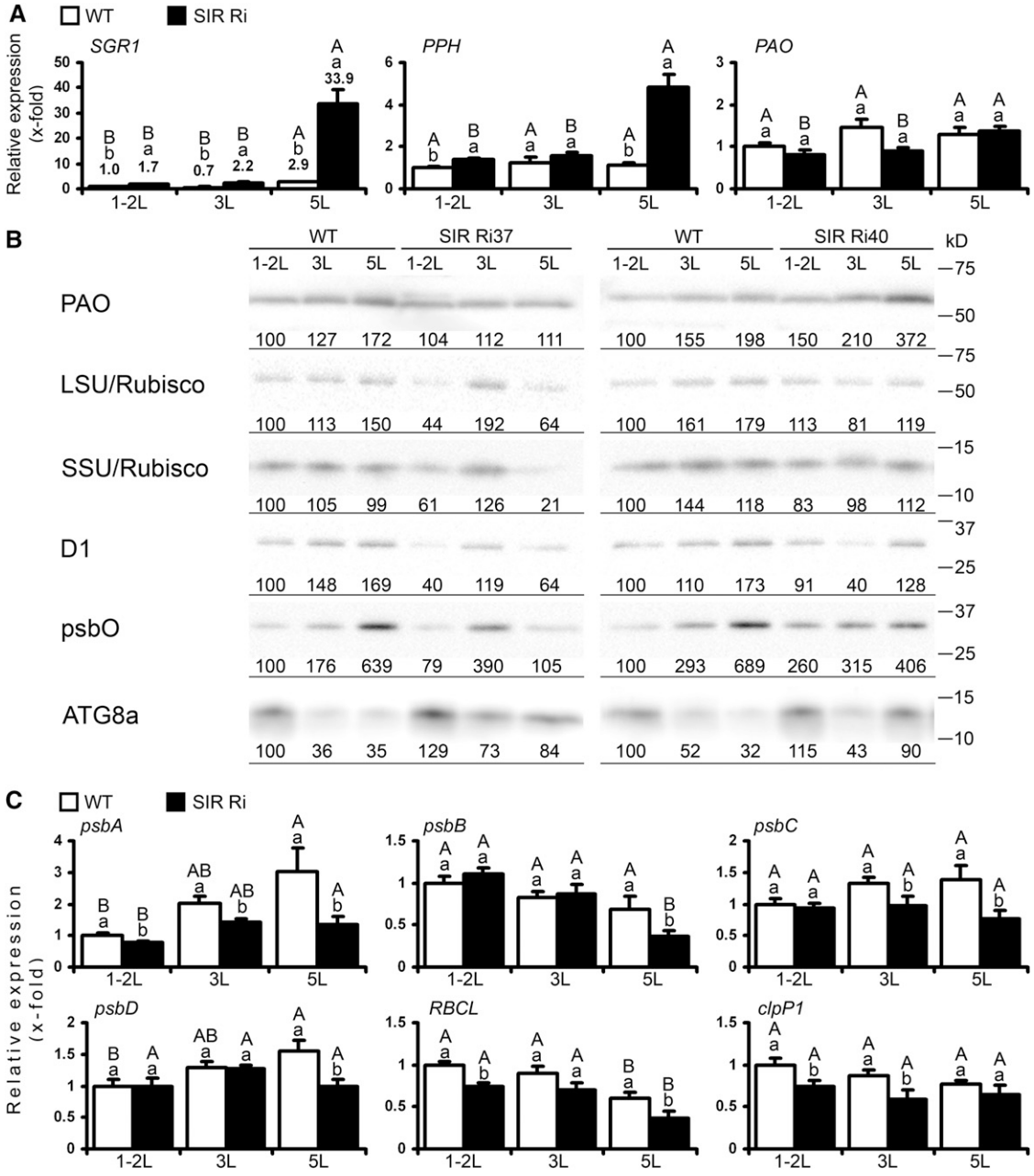

Figure 2. The expression of plastidic transcripts and proteins in wild-type (WT) and SIR Ri plants at the age of 1 month. A, Expression of genes related to chlorophyll degradation in SIR Ri plants. The top (1-2L), the third (3L), and the fifth (5L) leaves (counted from the tops) were collected and analyzed by quantitative real-time PCR using *TFIID* (*SGN-U571616*) as a housekeeping gene. The values are average ± SE ($n = 8$ for the wild type and SIR Ri [presented as average ± SE of SIR Ri37 and SIR Ri40]). The values were normalized to the top leaf of the wild type. B, Immunoblotting analysis of wild-type and SIR Ri tomato plants. Leaf samples were collected according to their positions from the plant tops. Extracted proteins were separated using SDS-PAGE, transferred to polyvinylidene difluoride membranes, and incubated with protein-specific antibodies as described in "Materials and Methods." Protein extracts were loaded as 0.5 μg per lane for D1, psbO (one of the subunits that construct the water-splitting system of PSII), and Rubisco (LSU and SSU) or 10 μg per lane for PAO and ATG8a. Relative band intensities are shown normalized to the top leaves of the wild-type plants. The positions of Precision Plus Protein Standards (Bio-Rad) are shown. C, Expression of genes encoded by chloroplast genome. Quantitative real-time PCR analysis was performed as described in A. The values denoted by different letters are significantly different according to the Tukey-Kramer honestly significant difference mean-separation test (JMP 8.0; $P < 0.05$). The uppercase letters reflect differences between leaves of the same genotype; the lowercase letters distinguish different genotypes.

total glutathione, sulfite was increased in the top third and fifth leaves of 1-month-old SIR Ri plants compared with wild-type leaves (Fig. 3B).

Sulfide in plant cells can be generated either as the result of sulfite reduction by SiR in chloroplasts (Yi et al., 2010; Takahashi et al., 2011) or the release from degraded sulfur-containing biomolecules such as Cys (Alvarez et al., 2010; Álvarez et al., 2012). While sulfide was decreased with leaf age in wild-type leaves, in SIR Ri plants, it increased with leaf age. Accordingly, sulfide levels were lower in the top leaves of SIR Ri plants than in the wild type and similar in the third leaves of both genotypes. However, the lower fifth leaves of SIR Ri plants showed significantly higher sulfide than the wild type (Fig. 3B, left insert in the middle). The relatively high sulfide levels detected in the third and fifth leaves in SIR Ri plants indicate that the decreased sulfide synthesized by the impaired SiR activity in these leaves was most likely compensated by sulfide originated from the degradation of sulfur-containing metabolites, e.g. free and protein-bound sulfur amino acids and glutathione. Free Cys levels followed the same trend as sulfide and were increased with leaf age in SIR Ri plants, being lower than the wild type in the top leaves, similar in the third leaf, and higher than the wild type in the fifth leaf (Fig. 3B, middle insert in the middle). The decreased levels of sulfide, Cys, and total glutathione in the top leaves of SIR Ri plants unequivocally indicate the impairment of the sulfate assimilation reductive pathway due to limited SiR activity.

Thiosulfate can be a product of sulfite detoxification in plants, as it is considered to be less toxic than sulfite (Tsakraklides et al., 2002; Brychkova et al., 2013). Sulfite accumulation in SiR-impaired plants was accompanied by significantly higher levels of thiosulfate than detected in leaves of the wild type, approximately 1.4- to 2.0-fold higher levels in all the leaves of the 1-month-old SIR Ri tomato plants compared with the wild-type plants (Fig. 3B). The pathway of sulfolipid biosynthesis provides an additional route for sulfite detoxification, as it consumes sulfite for the reaction with UDP-Glc (Sanda et al., 2001; Shimojima, 2011). As a possible consequence of the sulfite enhancement in SiR-impaired plants, the top and the third leaves of SIR Ri plants had significantly higher SQDG content than the corresponding leaves of the wild type (Fig. 3B). However, while SQDG did not alter with leaf age in

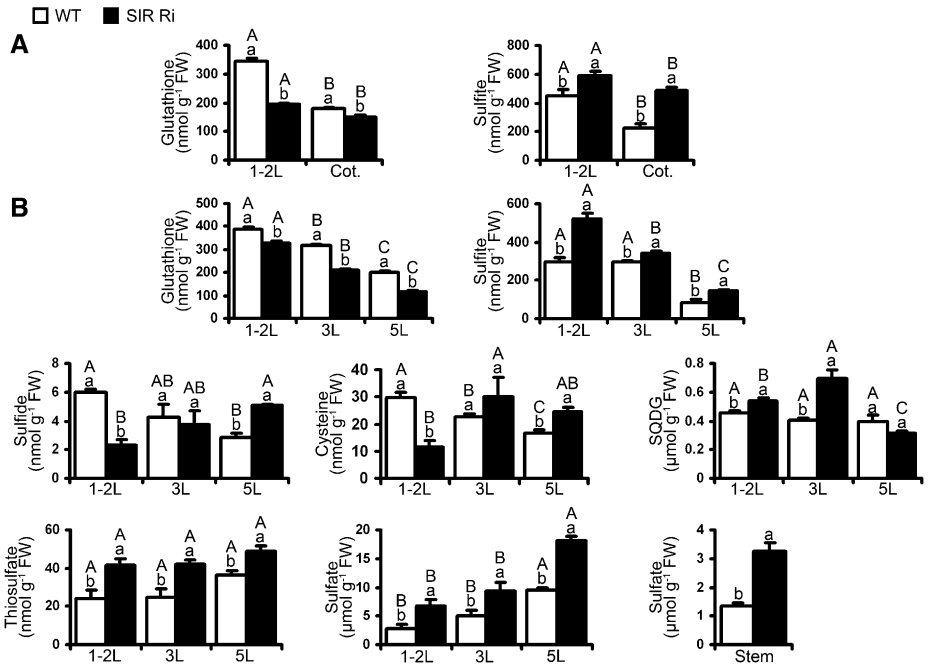

Figure 3. The effect of SiR impairment on sulfur metabolite levels in different tomato leaves. A, Glutathione (left) and sulfite (right) in the 2-week-old tomato plants. The metabolites were detected in cotyledons (Cot.) and the top leaves (1-2L) of SIR Ri and wild-type (WT) plants. The presented values are average ± SE ($n = 4$ for glutathione and $n = 6$ for sulfite assays). B, Sulfur metabolites in leaves of 1-month-old SIR Ri and wild-type plants. The top (1-2L), the third (3L), and the fifth (5L) leaves (counted from the tops) were collected; glutathione, sulfite, sulfide, Cys, SQDG, thiosulfate, and sulfate were quantified in the samples as described in "Materials and Methods." The presented values are average ± SE (each metabolite was quantified in three to six technical repeats). The stem segments were collected between the ground and cotyledons. The presented values are average ± SE ($n = 3$). The values denoted by different letters are significantly different according to the Tukey-Kramer honestly significant difference mean-separation test (JMP 8.0; $P < 0.05$). The uppercase letters reflect differences between leaves of the same genotype; the lowercase letters distinguish different genotypes.

wild-type plants, the fifth leaves of the 1-month-old SIR Ri plants contained significantly less SQDG than the upper leaves of the same plants, indicating that the increased sulfolipid degradation with leaf age paralleled the senescence symptoms in SIR-impaired plants (Fig. 3B).

Sulfate was dramatically enhanced in all the leaves of SIR Ri plants, ca 2-fold higher than in wild-type leaves (Fig. 3B; Supplemental Fig. S5). Sulfate enhancement could be the result of sulfite oxidation in the leaves and/or enhanced sulfate uptake. The higher total sulfur concentrations detected in the mutant leaves (Supplemental Fig. S6) and the increased sulfate in the lower stem segment in SIR Ri plants indicate that SiR impairment resulted in enhanced sulfate uptake compared with wild-type plants (Fig. 3B). Importantly, while the upper leaves of the mutants showed only an insignificant influx of total sulfur and a slight reduction of organic sulfur (calculated as a subtraction of sulfate and sulfite from the total sulfur), total sulfur was significantly enhanced in the fifth leaf of SIR Ri plants compared with the wild type (Supplemental Fig. S6). Sulfate prevailed in the total sulfur pool of the fifth yellowing leaf of SIR Ri plants (89% $\pm$ 4%), whereas organic sulfur in these leaves was approximately 2.7-fold lower than in the wild type (Supplemental Fig. S6), reflecting a vast degradation of sulfur-containing organic substances.

Sulfite Homeostasis in SiR-Impaired Tomato Plants

Increased concentrations of sulfite were shown previously to cause leaf damage (Brychkova et al., 2013). The expression of the sulfite network transcripts and enzymes was generally affected by leaf age and genotype of the plants, in a manner similar to the distribution of sulfur metabolites (Figs. 4 and 5; Supplemental Figs. S7 and S8). As expected, *SiR* transcript (by more than 2-fold) and SiR activity (by 1.5- to 1.8-fold) levels were higher in the wild type than in SiR mutants and decreased with leaf age (Figs. 4 and 5; Supplemental Figs. S7 and S8). While *SO* transcript in the wild-type plants was not affected by leaf age, its expression was unexpectedly lower in the fifth leaves of SIR Ri mutants compared with the upper leaves of the mutant and the fifth leaves of wild-type plants (Fig. 4, top middle insert). However, despite the lower transcript level, SO activity was dramatically increased in the fifth leaf, indicating a process of posttranscriptional control. SO activity increased with leaf age, likely as a result of increased cellular sulfite. This increase occurs due to the natural reduction in SiR activity with age in wild-type plants and due to the forced reduction in SiR-impaired plants (Fig. 5; Supplemental Fig. S8). Accordingly, the enhanced activity of SO in SiR-impaired plants is in agreement with the higher sulfate levels in the leaves of SIR Ri plants compared with wild-type leaves.

The increased sulfite in the leaves of SiR-impaired plants could be a result of the reduced SiR activity coupled to enhanced APR expression. Enhanced expression of the APR transcripts as well as enhanced APR activity were evident in SiR-impaired plants compared with the corresponding leaves in wild-type plants at the age of 1 and 2 months (Figs. 4 and 5; Supplemental Figs. S7 and S8). The notion regarding enhanced APR-dependent sulfite generation in SIR Ri plants was supported by the enhanced ATPS activity in SiR-impaired plants, especially in the lowest leaves, being able to generate enough APS, the substrate for sulfite generation by APR (Fig. 5, bottom left insert).

Thiosulfate accumulation in plants may indicate excessive sulfite conversion to the less toxic thiosulfate by the STs activity (Brychkova et al., 2013). Net ST activity in plants was defined as the difference between detected sulfite generation and consumption (Brychkova et al., 2013). Net ST activity was enhanced with leaf age in both genotypes. In SIR Ri plants, only the activity of the top leaf was found to be higher than that of the corresponding wild-type leaves, while in the third and fifth leaves, activity was significantly lower or tended to be lower than the corresponding leaves of the wild-type plants (Fig. 5). Taking into account that thiosulfate content was higher in SIR Ri than in the wild-type plants (Fig. 3) and that the sulfite detoxification activity of STs was enhanced only in the top leaves of SIR Ri plants (Fig. 5), these results indicate that the thiosulfate increase in SiR-impaired plants was likely related to other ST activities (Papenbrock et al., 2011) that were not detected here.

Interestingly, although the transcript of SQD1 protein, which directs sulfite to the sulfolipid biosynthesis pathway (Sanda et al., 2001), was not affected (Fig. 4), the SQDG content was significantly enhanced in the young leaves of SIR Ri plants compared with wild-type young leaves (Fig. 3B). However, the increased sulfite incorporation into SQDG was not sufficient to maintain low basal sulfite levels (Fig. 3).

Considering the expression of the sulfite network components and sulfur-containing metabolites in SIR Ri tomato plants, our results indicate that SiR impairment results in a thiol shortage that activates the sulfate reduction pathway, including APR-generated sulfite (Leustek et al., 2000; Kopriva and Rennenberg, 2004; Kopriva, 2006). In the absence of normal SiR activity, the other sulfite-converting components of the sulfite network are activated for maintaining homeostatic sulfite levels in the plant tissues.

DISCUSSION

Formation of Sulfite by APR in SiR-Impaired Plants

Our results show that a reduction in SiR to approximately 50% to 65% of the wild-type SiR activity (Fig. 5; Supplemental Fig. S8) resulted in multiple phenotypes, including a reduction in total organic sulfur and glutathione in plant leaves, increased sulfite and sulfate, and premature senescence (Figs. 1 and 3; Supplemental Figs. S1–S3, S5, and S6). Moreover, despite the reduced ability to utilize sulfite, the tomato plants with impaired

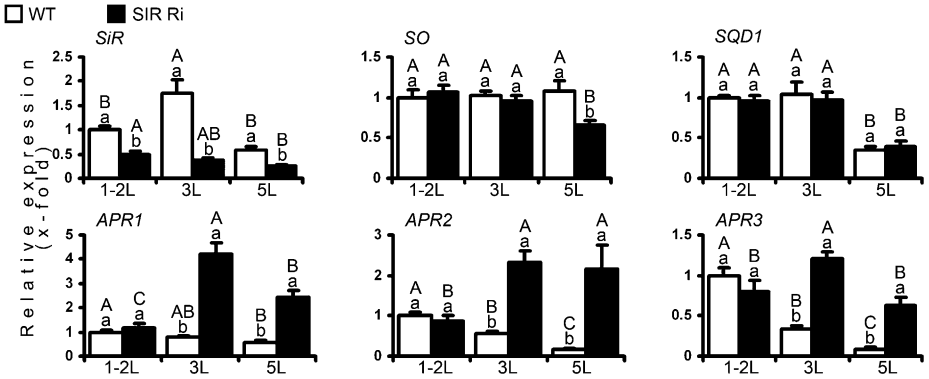

Figure 4. The impact of SiR suppression on transcripts of the sulfite network genes. The top (1-2L), the third (3L), and the fifth (5L) leaves (counted from the tops) were collected from 1-month-old SIR Ri and wild-type (WT) plants and analyzed by quantitative real-time PCR using *TFIID* (*SGN-U571616*) as a housekeeping gene. The values are average ± SE ($n = 8$ for the wild type and SIR Ri [SIR Ri37 and SIR Ri40 plants were summarized together]). The values were normalized to the top leaves of the wild-type plants. The values denoted by different letters are significantly different according to the Tukey-Kramer honestly significant difference mean-separation test (JMP 8.0; $P < 0.05$). The uppercase letters reflect differences between leaves of the same genotype; the lowercase letters distinguish different genotypes.

SiR exhibited enhanced APR expression in all their leaves compared with the corresponding wild-type leaves (Figs. 4 and 5; Supplemental Figs. S7 and S8). The insufficient accumulation of reduced sulfur products in SIR-impaired plants seems also to result in elevated sulfate uptake by roots (Khan et al., 2010) and enhanced transportation of sulfate in stems (Fig. 3B). The net result is that the accumulation of sulfite (Fig. 3) as the enhanced APR activity was further exacerbated by the increased activity of ATPS, which catalyzes the biosynthesis of APS, the substrate for APR, being significantly higher in the fifth leaf of the mutant plants (Fig. 5). The result is unexpected, as chloroplastic APR is accepted as the main regulatory point in the sulfate assimilation reductive pathway (Vauclare et al., 2002). Yet, as our results show, no direct product feedback mechanism exists for this metabolic stage. APR is known to be regulated by a number of factors such as diurnal rhythm (Kopriva et al., 1999), nitrogen deficiency (Kopriva et al., 2002), and carbohydrate (Hesse et al., 2003) and salinity levels (Koprivova et al., 2008). Importantly, APR is highly regulated by thiols in a demand-driven manner (Leustek et al., 2000; Kopriva and Rennenberg, 2004; Kopriva, 2006), i.e. its activity increases when reduced sulfur compounds levels are low, such as during sulfur starvation or depletion of glutathione, and decreases when excess reduced sulfur is available (Vauclare et al., 2002; Kopriva and

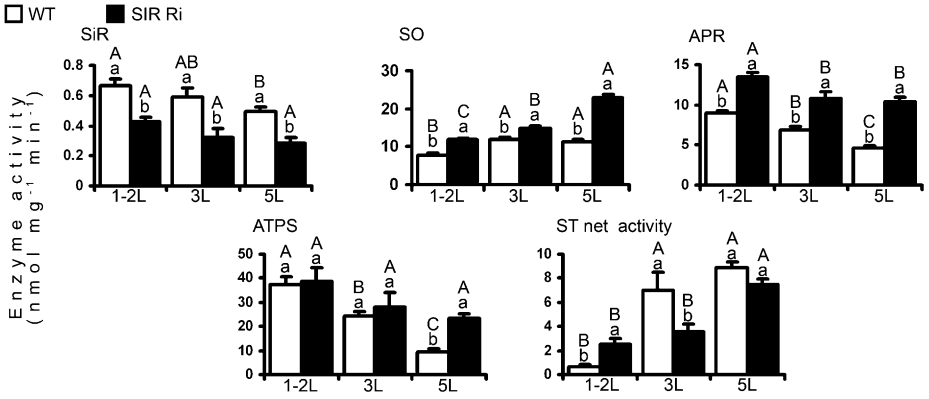

Figure 5. Effect of SiR impairment on the sulfite network enzyme activities. The top (1-2L), the third (3L), and the fifth (5L) leaves (counted from the tops) were collected from 1-month-old SIR Ri and wild-type (WT) tomato plants; enzyme assays in the leaves were performed as described in "Materials and Methods." The presented values are average ± SE ($n = 3$), where data for SIR Ri plants represent the average of the activities detected in SIR Ri37 and SIR Ri40 plants. ATPS activity is expressed as nmol ATP mg^{-1} protein min^{-1}, SiR activity is expressed as nmol Cys mg^{-1} protein min^{-1}, and SO, ST, and APR activities are expressed as nmol sulfite mg^{-1} protein min^{-1}. The values denoted by different letters are significantly different according to the Tukey-Kramer honestly significant difference mean-separation test (JMP 8.0; $P < 0.05$). The uppercase letters reflect differences between leaves of the same genotype; the lowercase letters distinguish different genotypes.

Koprivova, 2004; Kopriva, 2006; Davidian and Kopriva, 2010). Thus, it is not the lack of sulfide that causes physiological damage but rather the condition in which thiol demand-driven positive regulation of chloroplastic APR obviates its control by excess sulfite product.

Direct deregulation of APR activity has been achieved in Arabidopsis and maize (*Zea mays*) mutants by overexpression of APR from *Pseudomonas aeruginosa* (PaAPR). The resultant plants exhibited stunted growth, leaf chlorosis, and sectoring with nonchlorophyll tissue, as compared with the wild type (Tsakraklides et al., 2002). In that case, the activity of PaAPR was several-fold higher than the native APR activity in maize (Martin et al., 2005) and Arabidopsis (Tsakraklides et al., 2002) wild-type plants. The PaAPR overexpression resulted in relatively low accumulation of toxic sulfite (up to 120 nmol g^{-1} fresh weight [FW] higher than the wild type; Tsakraklides et al., 2002). Nonetheless, the damages resembled SO_2-induced lesions (Martin et al., 2005) and are likely the result of long-term sulfite toxicity, whose level exceeded the capacity of the sulfite network to convert sulfite to less toxic metabolites (Tsakraklides et al., 2002). SO-impaired Arabidopsis plants, fumigated with a relatively low SO_2 concentration (0.6 μL L^{-1}), which did not damage wild-type plants, exhibited typical sulfite-induced damages only after a relatively long time (60 h) of exposure (Randewig et al., 2012). Thus, the PaAPR-induced damage in Arabidopsis and maize plants (Tsakraklides et al., 2002; Martin et al., 2005) and the long-term induced damage by relatively low SO_2 are in agreement with our results showing that enhanced APR and impaired SiR activity result in sulfite accumulation, damage to chloroplasts, and premature senescence (Figs. 1–5; Supplemental Figs. S1, S2, S4, S7, and S8).

Glutathione levels in SiR-impaired leaves could be depleted not only by the reduced sulfide supply for Cys biosynthesis, a component of the glutathione tripeptide, but also by direct interaction of sulfite with glutathione by a nucleophilic displacement mechanism to form thiol and *S*-sulfonate compounds (Stricks et al., 1955). A fast (within 3 h) glutathione decrease was evident in Arabidopsis wild-type and SiR-impaired leaves in response to application of sulfite (Yarmolinsky et al., 2013) and in rat hepatocytes where sulfite cytotoxicity was accompanied by a rapid disappearance of oxidized glutathione followed by a slow depletion of glutathione (Niknahad and O'Brien, 2008). Accordingly, tobacco (*Nicotiana tabacum*) and poplar (*Populus* spp.) plants overexpressing Cys synthase and exhibiting enhanced glutathione biosynthesis were highly resistant to sulfite (Noji et al., 2001; Nakamura et al., 2009), and Arabidopsis plants overexpressing SiR were resistant to sulfite toxicity, likely as the result of glutathione accumulation in response to sulfite injection (Yarmolinsky et al., 2013). The resistance to sulfite in the plants containing high glutathione levels can be attributed to the role of glutathione in protecting leaves from sulfite-induced oxidative stress (Noji et al., 2001; Nakamura et al., 2009) and/or by a direct interaction with sulfite.

The changes in sulfite and glutathione are both expected to affect APR activity in opposing ways. Exogenous sulfite applications were shown to suppress APR activity (Randewig et al., 2012; Brychkova et al., 2013), whereas a decrease of thiol in plants enhanced sulfate assimilation by the activation of APR expression (Vauclare et al., 2002; Kopriva and Koprivova, 2004; Kopriva, 2006; Davidian and Kopriva, 2010). In our study, the level of APR expression, which was higher in SIR Ri leaves compared with the leaves of the wild-type plants, indicates that the APR induction by glutathione depletion overcame the APR suppression, inducing a dangerous cycle of further sulfite enhancement. Taken together, our results indicate that SiR impairment shows that the senescence-like phenotype is consistent with damage caused by sulfite. Furthermore, decreased glutathione in SiR-impaired plants as a result of the biosynthetic lesion led to unexpected enhanced futile APR expression and further sulfite overproduction.

SiR Activity and Sulfite Homeostasis Impacts on Leaf Senescence

Sulfite is a toxic intermediate in the plant sulfate reductive pathway, and therefore, its level is tightly regulated (Tsakraklides et al., 2002; Brychkova et al., 2013). The detoxifying capability of SO has been demonstrated to be an important component of the sulfite network, protecting plants against sulfite toxicity (Brychkova et al., 2007, 2013; Lang et al., 2007). In view of the K_m value of SiR for sulfite being comparable to that of SO, 10 μM (Krueger and Siegel, 1982) versus 33.8 μM (Eilers et al., 2001), respectively, it is reasonable to expect a role of SiR in the efficient utilization of excessive sulfite, at least, in the chloroplasts where SiR is localized. The importance of SiR in plant protection from sulfite toxicity was highlighted in Arabidopsis and tomato plants with a partial suppression of SiR activity. In that case, the plants are more sensitive to toxic sulfite than wild-type plants (Yarmolinsky et al., 2013).

Importantly, leaves of SIR Ri plants contained significantly higher sulfite levels than the corresponding leaves of the wild-type plants (Fig. 3). The endogenous sulfite levels detected in SIR Ri top leaves (593 and 522 nmol sulfite g^{-1} FW in 2-week-old and 1-month-old plants, respectively) are at a similar level to the sulfite detected in SIR Ri mutant leaves injected with 4 mM sulfite (i.e. resulting in 632 and 520 nmol sulfite g^{-1} FW 30 min and 24 h after the injection, respectively; Yarmolinsky et al., 2013). Considering the damage caused by the similar levels of injected sulfite, these results indicate that the symptoms of early senescence detected in SIR Ri-impaired leaves can be attributed to the prolonged exposure to the toxic sulfite (Fig. 1; Supplemental Figs. S1 and S2). It is also possible that the actual level of sulfite that was produced in SIR Ri

plants was higher than what was detected here (Fig. 3) due to its fast reduction and oxidation and binding to tissue constituents (Huber et al., 1987; Papenbrock and Schmidt, 2000; Tsakraklides et al., 2002; Brychkova et al., 2012a; Yarmolinsky et al., 2013).

In addition to SiR, sulfite can be consumed by other enzymes of the sulfite network. Although the back oxidation of sulfite to sulfate was shown to be the main avenue in sulfite detoxification (Van Der Kooij et al., 1997; Brychkova et al., 2012a), the insufficient SiR activity resulted in high sensitivity of SiR-impaired plants to excessive sulfite, despite the up-regulated SO activity (Yarmolinsky et al., 2013). The enhanced SO activity is the primary response of the sulfite network, protecting plant cells from the prolonged excessive sulfite in the mutant leaves (Fig. 5; Supplemental Fig. S8; Khan et al., 2010; Yarmolinsky et al., 2013). However, due to the peroxisomal localization of SO, the chloroplast is especially prone to sulfite under conditions where SiR is disabled and APR activity continues. The net result is the initiation of premature leaf senescence, as was evident in the cotyledons and older leaves by yellowing, chlorophyll degradation, maximal quantum yield decrease, and the enhanced chloroplastic protein degradation (Figs. 1 and 2; Supplemental Figs. S1–S3).

SQD1 can potentially contribute to sulfite detoxification due to its low K_m value for sulfite (10 μM) and chloroplast localization (Sanda et al., 2001). SQDG, whose biosynthesis starts with SQD1 activity, was enhanced in the younger leaves of SIR Ri plants (Fig. 3B). Importantly, rapid up-regulation of SQD1 in response to sulfite injections has been noticed in tomato plants injected with sulfite solutions (Brychkova et al., 2013), supporting the notion of the participation of SQD1 in sulfite detoxification as a member of the sulfite network. However, SQD1 activity in SIR Ri plants was apparently insufficient to protect chloroplasts from sulfite. The increased SQDG level in the upper leaves of SIR Ri plants might be also related to additional stabilization of PSII (Minoda et al., 2002, 2003) required during enhanced sulfite production.

Taken together, our results suggest that SiR plays a central role in sulfite detoxification in the chloroplasts, guarding the organelle during an increase of APR activity and/or sulfite penetration from outside (Huber et al., 1987; Papenbrock and Schmidt, 2000; Tsakraklides et al., 2002; Brychkova et al., 2012a; Yarmolinsky et al., 2013). We further show that conversion of sulfite into sulfolipids and its oxidation into sulfate were not sufficient to maintain basal sulfite levels at nontoxic levels in SIR Ri plants.

Early Leaf Senescence in the Tomato SiR-Impaired Plants

Leaf senescence affects sulfur metabolism, and the levels of sulfur metabolites and enzyme activities related to sulfur metabolism largely depend on leaf age/positions (Figs. 3–5; Supplemental Figs. S7 and S8). Leaf senescence consists of highly regulated degradation of complex biomolecules in aged leaves and the remobilization of the released nutrients to newly formed sink organs, including young leaves and developing seeds (Guiboileau et al., 2010). This process is tightly connected to plant response to stress, which can initiate premature leaf senescence (Gepstein and Glick, 2013). Here, we showed that SiR impairment is associated with deterioration of chloroplast performance, degradation of chlorophyll and protein, accumulation of autophagy ATG8a proteins, hydrogen peroxide, and lipid peroxidation products, which are all hallmarks of leaf senescence (Figs. 1 and 2; Supplemental Figs. S1–S3).

SiR-impaired plants were characterized by the accumulation of sulfate in the leaves (Fig. 3; Supplemental Fig. S5), which is considered as a trait of leaf senescence (Watanabe et al., 2013). The excessive sulfate in leaves is a result of the enhanced SO activity that produces sulfate de novo from sulfite generated by the enhanced APR activity (Fig. 5; Supplemental Fig. S8) and/or released from degraded sulfur-containing metabolites (Brychkova et al., 2013). The source for sulfite generation in the leaves by APR is likely the enhanced sulfate translocation from the lower plant parts of SiR-impaired plants, as was shown previously in Arabidopsis SiR mutants by Khan et al. (2010) and indicated here by the higher sulfate level in the lowest stems of SIR Ri compared with the wild type (Fig. 3B). The increased sulfate is the main source for the enhanced total sulfur in SIR Ri leaves (Supplemental Fig. S6).

Cys levels followed the same trend as sulfide and were increased with leaf age in SIR Ri plants, being lower than the wild type in the top leaves but similar and even higher than the wild-type third and fifth leaves, respectively (Fig. 3B, left and middle inserts of the middle section). Considering that the senescence symptoms appeared in the third and fifth leaves of SIR Ri37 and in the fifth leaf of Ri40 (Fig. 1B), as well as the decreased organic sulfur in the lower leaves of SIR Ri plants (Supplemental Fig. S6), the increase of Cys levels in the lower leaves of the mutant plants is likely a result of the accelerated catabolic processes that results in the degradation of sulfur-containing metabolites (Brychkova et al., 2013) and yellowing of the leaves (Fig. 5). Cys is the direct donor of sulfur atom for the maturation, by sulfuration, of the active center of the molybdo enzyme xanthine dehydrogenase (XDH), catalyzed by molybdenum cofactor sulfurase (ABA3 in Arabidopsis and FLACCA in tomato; Sagi et al., 1999, 2002; Bittner et al., 2001). Recently, it was shown that a shortage in Cys availability in the plant reduced the activity of XDH in Arabidopsis (Cao et al., 2014). XDH plays a pivotal role in purine catabolism, and impairment in XDH activity results in plant premature senescence (Brychkova et al., 2008). One may expect XDH activity to be decreased in the top leaves of SIR Ri plants, where lower Cys levels compared with the wild type were evident (Fig. 3). However, inspection of XDH activity revealed that XDH responded to factors other than Cys availability; in top and third leaves of SiR-impaired plants, the activity

was higher, whereas in the fifth leaf, it was similar, as compared with the wild type (Supplemental Fig. S9). The enhanced XDH activity in the top and third leaves compared with the wild type likely reflects senescence-related processes in these leaves, such as purine catabolism (Brychkova et al., 2008), and is in agreement with enhanced expression of ATG8a in SIR Ri compared with the wild type (Fig. 2). These results indicate that Cys level in mutant leaves did not limit XDH maturation by sulfuration and thus is not the cause for leaf senescence but rather the consequence of senescence-related processes in the mutant.

SiR impairment reduced photosynthesis efficiency, as follows from decreased quantum yield, affected chloroplast proteins (Figs. 1 and 2; Supplemental Figs. S1–S3), and deregulated carbon metabolism (Khan et al., 2010). The energy supply from the chloroplasts could be further significantly decreased by a futile cycle of sulfate reduction to sulfite followed by sulfite back oxidation to sulfate. Each round of this cycle would consume one ATP molecule for sulfate adenylation and two molecules of GSH for APS reduction to sulfite (Yi et al., 2010; Takahashi et al., 2011). Taking into account the simultaneous up-regulation of ATPS, APR, and SO in SiR-impaired leaves compared with wild-type plants, the futile cycle of sulfate reduction to sulfite followed by sulfite back oxidation to sulfate by SO in SiR-impaired plants could be an energetically costly process wasting ATP and GSH and enhancing the drop of glutathione levels in the mutant leaves (Fig. 3; Supplemental Fig. S5).

SiR Impairment Leads to Metabolic Block in Reduced Sulfur and Excess Sulfite That Are Responsible for the Premature Senescence

The toxicity of exogenous sulfite was shown to be dependent on the level of SiR expression in plants, indicating that SiR plays a role in protecting leaves against the toxicity of sulfite accumulation (Yarmolinsky et al., 2013). Here, we analyze different mutant plants at the steady state and detect endogenous sulfite levels in top leaves of tomato SIR Ri mutant that were previously shown to be above the threshold that causes damage. The increased sulfite oxidation to sulfate and incorporation of sulfite into SQDGs in mutant plants further indicate the important role of SIR in sulfite detoxification, since both metabolic pathways were able to partially substitute the impaired SIR in conversion of excess sulfite. Furthermore, the direct product of SO activity, sulfate, was increased in leaves, and its enhanced transportation in stems of mutant plants (Fig. 3; Supplemental Fig. S5) as well as the enhanced expression of ATPS both lead to the increase of APR (Figs. 3 and 5; Supplemental Fig. S8) and are hallmarks of enhancement of the sulfate reductive pathway as a result of metabolic block by SiR. Thus, both the impairment of SiR in detoxifying excess sulfite and the block that results in decrease in glutathione are the result of SiR impairment and are thus simultaneously responsible for sulfite accumulation and premature senescence phenotype in the mutant.

The Effect of SiR Impairment on Photosynthesis

Photosynthesis efficiency was demonstrated to be modified by the effect of SO_2/sulfite on photosynthetic electron transport, photophosphorylation, and CO_2 assimilation levels (Shimazaki and Sugahara, 1979; Cerović et al., 1982; Schmidt et al., 1990; Veeranjaneyulu et al., 1991; Wu et al., 2011). The response of the photosynthesis process to sulfite is well studied at the physiological level; however, little is known about the molecular mechanism/s of sulfite influence on the photosynthetic apparatus. For example, a decrease in the activity of PSII was observed in the photosynthetic electron transport system of chloroplasts isolated from *Spinacia oleracea* plants after fumigation with SO_2 (Shimazaki and Sugahara, 1979); however, a specific target for sulfite toxicity has not been discovered, though a varied sensitivity to sulfite can be expected among the chloroplastic proteins. Here, we show that D1 and psbO proteins were greatly decreased in lower leaves of SIR-impaired plants compared with the upper leaves of these plants (Fig. 2B; Supplemental Fig. S4B). D1, the primary target of light-induced irreversible oxidative damage (Mattoo et al., 1981; Ohad et al., 1990), seems to be a sulfite-sensitive photosynthetic component and may act as an indicator for plant sensitivity to sulfite because its level was decreased in wheat (*Triticum aestivum*) leaves subjected to low levels of SO_2 for 4 months (Ranieri et al., 1995). PsbO plays a crucial role in stabilization of PSII, and its down-regulation resulted in a decline of quantum yield in Arabidopsis mutant (Yi et al., 2005). Accordingly, the reduced quantum yield in the lower leaves of SiR-impaired plants compared with the wild type (Fig. 1; Supplemental Figs. S1 and S2) can be, at least partially, attributed to the decrease of psbO protein in these leaves (Fig. 2B; Supplemental Fig. S4B). Rubisco, the most abundant protein in green tissue (Bindschedler and Cramer, 2011), was decreased in the lower leaves compared with the wild type (Fig. 2B; Supplemental Fig. S4B). The degradation of Rubisco is a hallmark of senescent leaves, reflecting nutrient remobilization to young plant organs (Khanna-Chopra, 2012). The increased levels of sulfite and ROS in SIR Ri plants likely damaged Rubisco molecules, initiating their degradation (Fig. 2B; Supplemental Fig. S4B), as has been demonstrated for oxidative stress (Mehta et al., 1992; Khanna-Chopra, 2012).

SiR was identified as an abundant component of nucleoid structure in chloroplasts (Cannon et al., 1999; Sato et al., 2001; Chi-Ham et al., 2002; Sekine et al., 2002, 2007). Though the role of SiR in nucleoid functioning has not been finally clarified, it was shown that the silencing of SiR greatly affected the expression of chloroplast-encoded genes (Kang et al., 2010). Despite significantly lowered SiR expression in the young top leaves of SIR Ri plants compared with the wild type

(Figs. 4 and 5), these leaves showed only slight down-regulation of *psbA*, *LSU/Rubisco*, and *clpP1* transcripts, while *psbB-D* transcripts as well as chlorophyll content and maximal quantum yield remained unchanged (Figs. 1B and 2C). Likely, the SiR-dependent alterations in nucleoid structures in the young leaves of SIR Ri plants were not sufficient to affect photosynthesis activity in these leaves (Figs. 4 and 5). However, chloroplast-encoded transcripts were down-regulated in the lower senescent leaves of SIR Ri plants, indicating that chloroplast nucleoid structures were probably deregulated due to the insufficient SiR protein and additional unknown factors. It is possible that the long-term exposure to sulfite, especially in the older leaves, affected proteins encoded by the chloroplast genome in SIR-impaired tomato plants, likely by opening S-S bridges in their structures (Ziegler and Libera, 1975). However, the decreased chloroplast-encoded transcripts in SIR-impaired plants could be also a consequence of premature leaf senescence that was induced by the reduced SiR activity.

A Role for ROS in Premature Senescence of SiR-Impaired Leaves

Sulfite accumulation that occurred during fumigation of plants and isolated chloroplasts with 2 ppm SO_2 led to the generation of hydrogen peroxide by a chain reaction, depending on photosynthetic electron transport and resulting in the oxidation of enzymes of the Calvin cycle as well as a decrease in photosynthesis rate (Asada and Kiso, 1973; Tanaka et al., 1982a, 1982b). Therefore, the higher hydrogen peroxide concentrations in the lower leaves of SiR-impaired plants (Supplemental Fig. S3) could be a result of sulfite accumulation in these leaves (Fig. 3). The development of early senescence in the lower leaves of SiR-impaired plants can be also attributed to the excess hydrogen peroxide (Supplemental Fig. S3) damaging plant structures (Cohen et al., 2005; Muthuramalingam et al., 2013) and/or acting as a signal molecule in senescence (Khanna-Chopra, 2012).

The accumulation of hydrogen peroxide may also be a consequence of the GSH level weakening the antioxidant capacity in these leaves and resulting in the accumulation of hydrogen peroxide (Supplemental Fig. S3). This notion is supported by the over-accumulation of hydrogen peroxide in Arabidopsis plants that were impaired in cytoplasmic *O*-acetyl-Ser (thiol)lyase activity and demonstrated GSH (López-Martín et al., 2008).

The oxidation of sulfite in plants is mainly attributed to SO activity (Eilers et al., 2001; Brychkova et al., 2007, 2012a; Lang et al., 2007). However, 40% of sulfite oxidation in nonstressed, nongreen suspension cultures of tobacco mutants lacking active SO was carried out by component/s other than SO (Eilers et al., 2001). Moreover, tomato and Arabidopsis RNA interference mutants lacking SO activity still exhibited significant residual sulfite oxidation (Eilers et al., 2001; Brychkova et al., 2007). The non-SO oxidation of sulfite was suggested to be initiated by ROS (Pfanz and Oppmann, 1991; Miszalski and Ziegler, 1992; Brychkova et al., 2012a; Hamisch et al., 2012). The decreased level of hydrogen peroxide, which was detected in the upper young leaves of SiR-impaired plants, could be a result of direct oxidation of sulfite to sulfate by hydrogen peroxide (Hänsch et al., 2006).

CONCLUSION

We show here how the impairment in SiR ability to reduce sulfite to sulfide results in deregulation of the sulfate assimilation reductive pathway as the result of decreased production of thiols in SiR-impaired plants. This is characterized by the enhancement of sulfate assimilation and sulfite overproduction (Figs. 3–5; Supplemental Figs. S5–S8). The increase of sulfite oxidation to sulfate and incorporation of sulfite into SQDGs were not sufficient to maintain nontoxic basal sulfite levels, resulting in accumulative leaf damage in SIR Ri plants as a consequence of sulfite toxicity. In addition to the higher sulfite levels, the lower glutathione versus higher hydrogen peroxide and MDA levels, which are hallmarks of oxidative stress, also likely further contributed to chlorophyll degradation and the early leaf senescence in the mutant plants. Our results add substantive understanding to the interplay of sulfur biosynthetic and breakdown pathways and clearly indicate that SiR expression is an essential tool for regulation of toxic sulfite during sulfate assimilation and should be properly expressed to avoid premature senescence in tomato leaves.

MATERIALS AND METHODS

Growth Conditions

Tomato (*Lycopersicon esculentum/Solanum lycopersicum* 'Rheinlands Ruhm') plants were germinated on filter papers, soaked with water, and transferred at the stage of cotyledons to pots filled with a peat and vermiculite (4:1, v/v) mixture containing slow-release high-N Multicote 4 with microelements (0.3% [w/w]; Haifa Chemicals, http://www.haifachem.com/). Tomato plants were grown in a growth room under a 12-h light/12-h dark regime, 22°C, 75% to 85% relative humidity, and 100 μmol m^{-2} s^{-1} light intensity. All plants in pots were supplemented with 20-20-20 (Haifa Chemicals) water-soluble fertilizer (1 g L^{-1}) once a week. Wild-type, SIR Ri37, and SIR Ri40 plants were vegetatively propagated in a controlled greenhouse under light intensity of 400 to 500 μmol m^{-2} s^{-1} at Ben-Gurion University, Sede Boqer Campus (Supplemental Fig. S1B).

SiR-Impaired Tomato Plants

Tomato SIR Ri lines with reduced SiR expression described recently (Brychkova et al., 2012c; Yarmolinsky et al., 2013) were employed in this study. The homozygous SIR Ri40-38 line (designated as SIR Ri40) carried one insertion of transfer DNA (Yarmolinsky et al., 2013), while SIR Ri37 line carried at least two insertions of transfer DNA in its genome and was amenable only for vegetative propagation (Yarmolinsky et al., 2013). However, using a large number of seeds, we could grow SIR Ri37 plants sufficient for demonstrating alterations from the wild type and similarity to SIR Ri40 plants in senescence symptoms, enzyme activities, proteins, transcripts, and metabolites

levels. Vegetative propagated wild-type, SIR Ri37, and SIR Ri40 plants were employed in this study to demonstrate earlier leaf senescence in 3-month-old SiR mutant plants (Supplemental Fig. S1B), while seed-propagated plants were used for all the other data presented. No difference was observable between the two plant sources.

We compared SIR Ri with wild-type leaves at different stages of development. Because of the early abscission of lower leaves in 2- and 3-month-old SIR Ri plants, the leaves were counted from the tops of both mutants and wild-type plants. For 1-month-old plants, where SIR Ri and wild-type plants had the same number of leaves, the following wild-type leaves were compared with the corresponding SIR Ri leaves: the first and second undeveloped leaves as counted from the top and the third and fifth leaves from the top (corresponding to the sixth and seventh and fifth and third leaves counted from the ground, respectively). For the 2- or 3-month-old plants, we compared the third, fifth, and seventh or third and sixth wild-type leaves, respectively, to the corresponding SIR Ri leaves. Three distal leaflets of the tomato leaves were collected from four to five tomato plants, shredded by scissors, well mixed, and frozen in liquid nitrogen. The samples were stored at –80°C until RNA, protein, or metabolite extraction.

Characterization of Photosynthesis in Tomato Plants

F_v/F_m was measured using a MiniPAM Photosynthesis Yield Analyzer (Heinz Walz) in tomato leaves adapted to dark for 20 min. Imaging of F_v/F_m was performed by using IMAGING-PAM M-Series in the MAXI Version (Heinz Walz). Chlorophyll was extracted from plant tissues in 80% (v/v) ethanol and detected as described by Brychkova et al. (2007). Chlorophyll was measured as the sum of chlorophyll *a* and *b* according to the following formula: $(13.7 \times A_{665} - 5.76 \times A_{649}) + (-7.60 \times A_{665} + 25.8 \times A_{649}$; Knudson et al., 1977).

Western-Blot Analysis

Proteins were extracted in buffer containing 250 mM Tris-HCl (pH 8.48), 1.25 mM EDTA, 14 mM GSH, 4 mM dithiothreitol, 5 mM L-Cys, 0.5 mM sodium molybdate, and 400 mM Suc and separated in 12.5% or 15% (w/v) acrylamide gels by SDS-PAGE followed by transfer to polyvinylidene difluoride membranes. Lanes were loaded either with 10 μg of protein (for PAO, Fdx1, and ATG8a) or 0.5 μg (for D1, Lhcb1, psbO, and LSU/Rubisco and SSU/Rubisco proteins). Commercial primary antibodies produced by Agrisera AB were used in the following dilutions: D1 (AS05 084), 1:10,000; Lhcb1 (AS01 004), 1:2,000; ferredoxin (AS06 121), 1:2,000; psbO (AS06 142-33), 1:5,000; and PAO (AS11 1783), 1:5,000. ATG8a protein was detected by protein-specific antibodies (dilution, 1:1,000), which were supplied by Abcam. Antibodies simultaneously recognizing large and small subunits of Rubisco (dilution, 1:3,000) were a gift from Michal Shapira (Life Science Department, Ben-Gurion University of the Negev, Israel).

Preparation of RNA and Quantitative Real-Time Reverse Transcription-PCR

Aurum Total RNA Mini Kit and iScript cDNA Synthesis Kit (Bio-Rad) were used to extract RNA and prepare complementary DNA (cDNA) according to the manufacture's instructions. Contamination with genomic DNA was detected by quantitative real-time PCR with primers for *ACTIN Tom41* (SGN-U60480) using RNA and cDNA samples as templates. Samples of cDNA containing less than 0.05% genomic DNA were used for further analysis. The quantitative analysis of transcripts was performed as previously described (Brychkova et al., 2007) employing suitable primers (see Supplemental Table S1 for the list of primers used, their sequences, and the expected PCR product). Real-time PCR reactions were normalized using *Transcription factor IID* (*TFIID*; SGN-U329249) and *ACTIN Tom41* (SGN-U60480) as housekeeping genes, both yielding highly similar results. The data are presented as relative expression (means ± SE) to the top or the third leaves of the wild-type plants at the age of 1 or 2 months, respectively. All PCR fragments were extracted from agarose gels, purified, and sequenced for verification.

Sulfur Metabolites and Enzyme Activities

Determination of sulfite, Cys, total glutathione, sulfate, and total sulfur was performed as previously described (Brychkova et al., 2012a, 2013; Yarmolinsky et al., 2013). Sulfite was detected by using the commercial kit employing chicken SO (Brychkova et al., 2012a). Sulfide was extracted in 50 mM citric acid, 100 mM Na_2HPO4, and 1 mM salicylic acid, pH 5.0 in the ratio 1:40 and measured immediately by employing the microsensor ISO-H2S-100 for H_2S measurement connected to the TBR1025 analog system (World Precision Instruments). A calibration curve was plotted based on known sulfide concentrations and used to estimate sulfide content in tomato leaves. All measurements were performed promptly to ensure stability of sulfide in solutions. Soluble protein concentrations were determined using the Bio-Rad protein assay according to the manufacturer's instructions.

SiR, SO, ST, and APR activities were assessed as described previously (Brychkova et al., 2012b, 2012c, 2013). Net ST activity in plants was detected as the difference between sulfite generation and consumption (Brychkova et al., 2013). ATPS activity was determined by measuring the production of ATP from APS and pyrophosphate. ATP formation was detected by hexokinase, which produces D-Glc-6-P from D-Glc and ATP, and further by Glc-6-P dehydrogenase forming β-NADPH in presence of β-NADP and D-Glc-6-P (Robbins, 1962; Bernt and Bergmeyer, 1974). ATPS was expressed as nmol ATP mg^{-1} protein min^{-1}, SiR activity was expressed as nmol Cys mg^{-1} protein min^{-1}, and SO, ST, and APR activities were expressed as nmol sulfite mg^{-1} protein min^{-1}. Crude protein extraction and in-gel XDH activity assay were performed as previously described (Yesbergenova et al., 2005).

Extraction and Determination of Sulfolipids

Fresh leaves of tomato plants (350 mg) were immersed in 3 mL of 75°C preheated isopropanol with 0.01% (w/v) butylated hydroxytoluene and incubated at 75°C for 15 min. Thereafter, chloroform (1.5 mL) and water (0.6 mL) were added, and the sample was incubated at room temperature for 1 h. The lipid extract was transferred to a new tube, and the extraction procedure was repeated with 4 mL of chloroform:methanol (2:1) with 0.01% (w/v) butylated hydroxytoluene until plant tissues became white. Then, 1 mL of 1 M KCl was added to the combined extract; following centrifugation at 4,000*g* for 15 min, the upper phase was discarded. Lipids were separated by adding 2 mL of water, discarding the upper phase and dissolving the remainder polar lipid fraction in chloroform. The polar lipid fraction was separated on a TLC Silico60 plate in chloroform:methanol:water (65:25:4) solution for the first direction, followed by additional separation in chlorophorm:methanol:NH_4OH: isopropylamine (65:35:5:0.5) solution in the perpendicular direction. The plates were sprayed with 0.01% (w/v) primulin solution in acetone:water (60:40, v/v). The spots corresponding to sulfolipids were traced under UV light, collected and transmethylated with 2% (v/v) sulfuric acid in absolute methanol, and separated by hexane as previously described (Khozin et al., 1997). Sulfolipids were quantified using Trace GC Ultra (Thermo Scientific, http://www.thermoscientific.com/) as previously described (Khozin et al., 1997).

Histochemical Staining of Hydrogen Peroxide and Detection of MDA

Whole leaves were cut from tomato plants; their petioles were dipped in solutions of DAB (1 mg mL^{-1}, pH 5.0) and incubated under light for 4 h. The leaves were discolored in several washes of ethanol at 80°C and then photographed. The intensity of DAB staining was quantified by using ImageJ software (http://rsbweb.nih.gov/ij/). MDA was measured in leaves of tomato plants according to Heath and Packer (1968) and Hodges et al. (1999).

Statistical Analysis

ANOVA (Tukey-Kramer honestly significant difference mean-separation test) was used to compare multiple groups of samples (JMP 8.0 software, http://www.jmp.com/). The bands on SiR immunoblotting were analyzed with ImageJ software (http://rsbweb.nih.gov/ij/) in accordance with the developer's recommendations.

The manuscript is based on the experiments, which were repeated two to five times and gave similar reproducible results.

Supplemental Data

The following materials are available in the online version of this article.

Supplemental Figure S1. Early leaf senescence in SIR-impaired tomato plants at the ages of 2 and 3 months.

Supplemental Figure S2. The uneven decline of maximal quantum yield in leaves of SIR Ri plants.

Supplemental Figure S3. Enhanced markers of oxidative stress in SiR-impaired tomato plants.

Supplemental Figure S4. Expression of plastidic transcripts and proteins in wild-type and SIR Ri plants at the age of 2 months.

Supplemental Figure S5. Accumulation of total glutathione and sulfate in 2-month-old wild-type and SIR Ri tomato plants.

Supplemental Figure S6. Accumulation of total sulfur and organic sulfur in 1-month-old tomato plants.

Supplemental Figure S7. The impact of SiR suppression on transcripts of the sulfite network genes in 2-month-old SIR Ri tomato plants.

Supplemental Figure S8. The effect of SiR impairment on SiR, SO, and APR activities in 2-month-old tomato plants.

Supplemental Figure S9. The influence of SiR impairment on XDH activity in leaves of 1-month-old tomato plants.

Supplemental Table S1. List of primers used for quantitative real-time PCR.

ACKNOWLEDGMENTS

We thank Dr. Shimon Rachmilevitch and Liron Summerfield for helpful contributions to this research.

Received April 14, 2014; accepted June 30, 2014; published July 1, 2014.

LITERATURE CITED

Alvarez C, Calo L, Romero LC, García I, Gotor C (2010) An *O*-acetylserine (thiol)lyase homolog with L-cysteine desulfhydrase activity regulates cysteine homeostasis in Arabidopsis. Plant Physiol **152:** 656–669

Álvarez C, García I, Moreno I, Pérez-Pérez ME, Crespo JL, Romero LC, Gotor C (2012) Cysteine-generated sulfide in the cytosol negatively regulates autophagy and modulates the transcriptional profile in *Arabidopsis*. Plant Cell **24:** 4621–4634

Amtmann A, Armengaud P (2009) Effects of N, P, K and S on metabolism: new knowledge gained from multi-level analysis. Curr Opin Plant Biol **12:** 275–283

Asada K, Kiso K (1973) Initiation of aerobic oxidation of sulfite by illuminated spinach chloroplasts. Eur J Biochem **33:** 253–257

Bernt E, Bergmeyer HU (1974) Hexokinase. *In* HU Bergmeyer, ed, Methods of Enzyme Analysis. Academic Press, New York, pp 473–474

Bindschedler LV, Cramer R (2011) Quantitative plant proteomics. Proteomics **11:** 756–775

Bittner F, Oreb M, Mendel RR (2001) ABA3 is a molybdenum cofactor sulfurase required for activation of aldehyde oxidase and xanthine dehydrogenase in *Arabidopsis thaliana*. J Biol Chem **276:** 40381–40384

Brychkova G, Alikulov Z, Fluhr R, Sagi M (2008) A critical role for ureides in dark and senescence-induced purine remobilization is unmasked in the Atxdh1 Arabidopsis mutant. Plant J **54:** 496–509

Brychkova G, Grishkevich V, Fluhr R, Sagi M (2013) An essential role for tomato sulfite oxidase and enzymes of the sulfite network in maintaining leaf sulfite homeostasis. Plant Physiol **161:** 148–164

Brychkova G, Xia Z, Yang G, Yesbergenova Z, Zhang Z, Davydov O, Fluhr R, Sagi M (2007) Sulfite oxidase protects plants against sulfur dioxide toxicity. Plant J **50:** 696–709

Brychkova G, Yarmolinsky D, Fluhr R, Sagi M (2012a) The determination of sulfite levels and its oxidation in plant leaves. Plant Sci **190:** 123–130

Brychkova G, Yarmolinsky D, Sagi M (2012b) Kinetic assays for determining in vitro APS reductase activity in plants without the use of radioactive substances. Plant Cell Physiol **53:** 1648–1658

Brychkova G, Yarmolinsky D, Ventura Y, Sagi M (2012c) A novel in-gel assay and an improved kinetic assay for determining in vitro sulfite reductase activity in plants. Plant Cell Physiol **53:** 1507–1516

Cannon GC, Ward LN, Case CI, Heinhorst S (1999) The 68 kDa DNA compacting nucleoid protein from soybean chloroplasts inhibits DNA synthesis in vitro. Plant Mol Biol **39:** 835–845

Cao MJ, Wang Z, Wirtz M, Hell R, Oliver DJ, Xiang CB (2013) SULTR3;1 is a chloroplast-localized sulfate transporter in *Arabidopsis thaliana*. Plant J **73:** 607–616

Cao MJ, Wang Z, Zhao Q, Mao JL, Speiser A, Wirtz M, Hell R, Zhu JK, Xiang CB (2014) Sulfate availability affects ABA levels and germination response to ABA and salt stress in *Arabidopsis thaliana*. Plant J **77:** 604–615

Cerović ZG, Kalezić R, Plesničar M (1982) The role of photophosphorylation in SO_2 and SO_3^{2-} inhibition of photosynthesis in isolated chloroplasts. Planta **156:** 249–254

Chi-Ham CL, Keaton MA, Cannon GC, Heinhorst S (2002) The DNA-compacting protein DCP68 from soybean chloroplasts is ferredoxin: sulfite reductase and co-localizes with the organellar nucleoid. Plant Mol Biol **49:** 621–631

Cohen I, Knopf JA, Irihimovitch V, Shapira M (2005) A proposed mechanism for the inhibitory effects of oxidative stress on Rubisco assembly and its subunit expression. Plant Physiol **137:** 738–746

Davidian JC, Kopriva S (2010) Regulation of sulfate uptake and assimilation—the same or not the same? Mol Plant **3:** 314–325

Dhindsa RS, Plumb-Dhindsa P, Thorpe TA (1981) Leaf senescence: correlated with increased levels of membrane permeability and lipid peroxidation, and decreased levels of superoxide dismutase and catalase. J Exp Bot **32:** 93–101

Eilers T, Schwarz G, Brinkmann H, Witt C, Richter T, Nieder J, Koch B, Hille R, Hänsch R, Mendel RR (2001) Identification and biochemical characterization of *Arabidopsis thaliana* sulfite oxidase. A new player in plant sulfur metabolism. J Biol Chem **276:** 46989–46994

Gepstein S, Glick BR (2013) Strategies to ameliorate abiotic stress-induced plant senescence. Plant Mol Biol **82:** 623–633

Guiboileau A, Sormani R, Meyer C, Masclaux-Daubresse C (2010) Senescence and death of plant organs: nutrient recycling and developmental regulation. C R Biol **333:** 382–391

Hamisch D, Randewig D, Schliesky S, Bräutigam A, Weber AP, Geffers R, Herschbach C, Rennenberg H, Mendel RR, Hänsch R (2012) Impact of SO_2 on *Arabidopsis thaliana* transcriptome in wild-type and sulfite oxidase knockout plants analyzed by RNA deep sequencing. New Phytol **196:** 1074–1085

Hänsch R, Lang C, Riebeseel E, Lindigkeit R, Gessler A, Rennenberg H, Mendel RR (2006) Plant sulfite oxidase as novel producer of H_2O_2: combination of enzyme catalysis with a subsequent non-enzymatic reaction step. J Biol Chem **281:** 6884–6888

Heath RL, Packer L (1968) Photoperoxidation in isolated chloroplasts. I. Kinetics and stoichiometry of fatty acid peroxidation. Arch Biochem Biophys **125:** 189–198

Hesse H, Trachsel N, Suter M, Kopriva S, von Ballmoos P, Rennenberg H, Brunold C (2003) Effect of glucose on assimilatory sulphate reduction in *Arabidopsis thaliana* roots. J Exp Bot **54:** 1701–1709

Hodges DM, DeLong JM, Forney CF, Prange RK (1999) Improving the thiobarbituric acid-reactive-substances assay for estimating lipid peroxidation in plant tissues containing anthocyanin and other interfering compounds. Planta **207:** 604–611

Hörtensteiner S, Kräutler B (2011) Chlorophyll breakdown in higher plants. Biochim Biophys Acta **1807:** 977–988

Huber K, Esterbauer H, Jäger HJ, Grill D (1987) Detection of sulphite in plants. Environ Pollut **46:** 127–136

Kang YW, Lee JY, Jeon Y, Cheong GW, Kim M, Pai HS (2010) In vivo effects of NbSiR silencing on chloroplast development in *Nicotiana benthamiana*. Plant Mol Biol **72:** 569–583

Keren N, Berg A, Levanon H, Ohad I, Ohad I, van Kan PJ (1997) Mechanism of photosystem II photoinactivation and D1 protein degradation at low light: the role of back electron flow. Proc Natl Acad Sci USA **94:** 1579–1584

Khan MS, Haas FH, Samami AA, Gholami AM, Bauer A, Fellenberg K, Reichelt M, Hänsch R, Mendel RR, Meyer AJ, et al (2010) Sulfite reductase defines a newly discovered bottleneck for assimilatory sulfate reduction and is essential for growth and development in *Arabidopsis thaliana*. Plant Cell **22:** 1216–1231

Khanna-Chopra R (2012) Leaf senescence and abiotic stresses share reactive oxygen species-mediated chloroplast degradation. Protoplasma **249:** 469–481

Khozin I, Adlerstein D, Bigongo C, Heimer YM, Cohen Z (1997) Elucidation of the biosynthesis of eicosapentaenoic acid in the microalga *Porphyridium cruentum*: II. Studies with radiolabeled precursors. Plant Physiol **114:** 223–230

Knudson LL, Tibbitts TW, Edwards GE (1977) Measurement of ozone injury by determination of leaf chlorophyll concentration. Plant Physiol **60:** 606–608

Kopriva S (2006) Regulation of sulfate assimilation in Arabidopsis and beyond. Ann Bot (Lond) **97:** 479–495

Kopriva S, Koprivova A (2004) Plant adenosine 5′-phosphosulphate reductase: the past, the present, and the future. J Exp Bot **55:** 1775–1783

Kopriva S, Muheim R, Koprivova A, Trachsel N, Catalano C, Suter M, Brunold C (1999) Light regulation of assimilatory sulphate reduction in *Arabidopsis thaliana*. Plant J **20:** 37–44

Kopriva S, Rennenberg H (2004) Control of sulphate assimilation and glutathione synthesis: interaction with N and C metabolism. J Exp Bot **55:** 1831–1842

Kopriva S, Suter M, von Ballmoos P, Hesse H, Krähenbühl U, Rennenberg H, Brunold C (2002) Interaction of sulfate assimilation with carbon and nitrogen metabolism in *Lemna minor*. Plant Physiol **130:** 1406–1413

Koprivova A, North KA, Kopriva S (2008) Complex signaling network in regulation of adenosine 5′-phosphosulfate reductase by salt stress in Arabidopsis roots. Plant Physiol **146:** 1408–1420

Krueger RJ, Siegel LM (1982) Spinach siroheme enzymes: isolation and characterization of ferredoxin-sulfite reductase and comparison of properties with ferredoxin-nitrite reductase. Biochemistry **21:** 2892–2904

Lang C, Popko J, Wirtz M, Hell R, Herschbach C, Kreuzwieser J, Rennenberg H, Mendel RR, Hänsch R (2007) Sulphite oxidase as key enzyme for protecting plants against sulphur dioxide. Plant Cell Environ **30:** 447–455

Leustek T, Martin MN, Bick JA, Davies JP (2000) Pathways and regulation of sulfur metabolism revealed through molecular and genetic studies. Annu Rev Plant Physiol Plant Mol Biol **51:** 141–165

López-Martín MC, Becana M, Romero LC, Gotor C (2008) Knocking out cytosolic cysteine synthesis compromises the antioxidant capacity of the cytosol to maintain discrete concentrations of hydrogen peroxide in Arabidopsis. Plant Physiol **147:** 562–572

Martin MN, Tarczynski MC, Shen B, Leustek T (2005) The role of 5′-adenylylsulfate reductase in controlling sulfate reduction in plants. Photosynth Res **86:** 309–323

Mattoo AK, Pick U, Hoffman-Falk H, Edelman M (1981) The rapidly metabolized 32,000-dalton polypeptide of the chloroplast is the "proteinaceous shield" regulating photosystem II electron transport and mediating diuron herbicide sensitivity. Proc Natl Acad Sci USA **78:** 1572–1576

Mehta RA, Fawcett TW, Porath D, Mattoo AK (1992) Oxidative stress causes rapid membrane translocation and in vivo degradation of ribulose-1,5-bisphosphate carboxylase/oxygenase. J Biol Chem **267:** 2810–2816

Minoda A, Sato N, Nozaki H, Okada K, Takahashi H, Sonoike K, Tsuzuki M (2002) Role of sulfoquinovosyl diacylglycerol for the maintenance of photosystem II in *Chlamydomonas reinhardtii*. Eur J Biochem **269:** 2353–2358

Minoda A, Sonoike K, Okada K, Sato N, Tsuzuki M (2003) Decrease in the efficiency of the electron donation to tyrosine Z of photosystem II in an SQDG-deficient mutant of *Chlamydomonas*. FEBS Lett **553:** 109–112

Miszalski Z, Ziegler H (1992) Superoxide dismutase and sulfite oxidation. Z Naturforsch **47:** 360–364

Muthuramalingam M, Matros A, Scheibe R, Mock HP, Dietz KJ (2013) The hydrogen peroxide-sensitive proteome of the chloroplast in vitro and in vivo. Front Plant Sci **4:** 54

Nakamura M, Kuramata M, Kasugai I, Abe M, Youssefian S (2009) Increased thiol biosynthesis of transgenic poplar expressing a wheat *O*-acetylserine(thiol) lyase enhances resistance to hydrogen sulfide and sulfur dioxide toxicity. Plant Cell Rep **28:** 313–323

Nakayama M, Akashi T, Hase T (2000) Plant sulfite reductase: molecular structure, catalytic function and interaction with ferredoxin. J Inorg Biochem **82:** 27–32

Niknahad H, O'Brien PJ (2008) Mechanism of sulfite cytotoxicity in isolated rat hepatocytes. Chem Biol Interact **174:** 147–154

Noji M, Saito M, Nakamura M, Aono M, Saji H, Saito K (2001) Cysteine synthase overexpression in tobacco confers tolerance to sulfur-containing environmental pollutants. Plant Physiol **126:** 973–980

Ohad I, Adir N, Koike H, Kyle DJ, Inoue Y (1990) Mechanism of photoinhibition in vivo. A reversible light-induced conformational change of reaction center II is related to an irreversible modification of the D1 protein. J Biol Chem **265:** 1972–1979

Papenbrock J, Guretzki S, Henne M (2011) Latest news about the sulfurtransferase protein family of higher plants. Amino Acids **41:** 43–57

Papenbrock J, Schmidt A (2000) Characterization of a sulfurtransferase from *Arabidopsis thaliana*. Eur J Biochem **267:** 145–154

Peltier JB, Ripoll DR, Friso G, Rudella A, Cai Y, Ytterberg J, Giacomelli L, Pillardy J, van Wijk KJ (2004) Clp protease complexes from photosynthetic and non-photosynthetic plastids and mitochondria of plants, their predicted three-dimensional structures, and functional implications. J Biol Chem **279:** 4768–4781

Pfanz H, Oppmann B (1991) The possible role of apoplastic peroxidases in detoxifying the air pollutant sulfur dioxide. *In* J Lobarzewski, H Greppin, C Penel, T Gaspar, eds, Biochemical, Molecular, and Physiological Aspects of Plant Peroxidases. University of Geneva, Geneva, pp 401–417

Pruzinská A, Tanner G, Anders I, Roca M, Hörtensteiner S (2003) Chlorophyll breakdown: pheophorbide a oxygenase is a Rieske-type iron-sulfur protein, encoded by the accelerated cell death 1 gene. Proc Natl Acad Sci USA **100:** 15259–15264

Randewig D, Hamisch D, Herschbach C, Eiblmeier M, Gehl C, Jurgeleit J, Skerra J, Mendel RR, Rennenberg H, Hänsch R (2012) Sulfite oxidase controls sulfur metabolism under SO_2 exposure in *Arabidopsis thaliana*. Plant Cell Environ **35:** 100–115

Ranieri A, Castagna A, Bini L, Soldatini GF (1995) Two-dimensional electrophoresis of thylakoid protein patterns in two wheat cultivars with different sensitivity to sulfur dioxide. Electrophoresis **16:** 1301–1304

Robbins PW (1962) Sulfate-activating enzymes. *In* SP Colowick, NO Kaplan, eds, Methods in Enzymology, Vol 5. Academic Press, New York, pp 964–977

Roberts IN, Caputo C, Criado MV, Funk C (2012) Senescence-associated proteases in plants. Physiol Plant **145:** 130–139

Roose JL, Yocum CF, Popelkova H (2010) Function of PsbO, the photosystem II manganese-stabilizing protein: probing the role of aspartic acid 157. Biochemistry **49:** 6042–6051

Sagi M, Fluhr R, Lips SH (1999) Aldehyde oxidase and xanthine dehydrogenase in a *flacca* tomato mutant with deficient abscisic acid and wilty phenotype. Plant Physiol **120:** 571–578

Sagi M, Scazzocchio C, Fluhr R (2002) The absence of molybdenum cofactor sulfuration is the primary cause of the *flacca* phenotype in tomato plants. Plant J **31:** 305–317

Sakuraba Y, Schelbert S, Park SY, Han SH, Lee BD, Andrès CB, Kessler F, Hörtensteiner S, Paek NC (2012) STAY-GREEN and chlorophyll catabolic enzymes interact at light-harvesting complex II for chlorophyll detoxification during leaf senescence in *Arabidopsis*. Plant Cell **24:** 507–518

Sanda S, Leustek T, Theisen MJ, Garavito RM, Benning C (2001) Recombinant Arabidopsis SQD1 converts udp-glucose and sulfite to the sulfolipid head group precursor UDP-sulfoquinovose in vitro. J Biol Chem **276:** 3941–3946

Sato N, Nakayama M, Hase T (2001) The 70-kDa major DNA-compacting protein of the chloroplast nucleoid is sulfite reductase. FEBS Lett **487:** 347–350

Schmidt W, Neubauer C, Kolbowski J, Schreiber U, Urbach W (1990) Comparison of effects of air pollutants (SO_2, O_3, NO_2) on intact leaves by measurements of chlorophyll fluorescence and P_{700} absorbance changes. Photosynth Res **25:** 241–248

Sekine K, Fujiwara M, Nakayama M, Takao T, Hase T, Sato N (2007) DNA binding and partial nucleoid localization of the chloroplast stromal enzyme ferredoxin:sulfite reductase. FEBS J **274:** 2054–2069

Sekine K, Hase T, Sato N (2002) Reversible DNA compaction by sulfite reductase regulates transcriptional activity of chloroplast nucleoids. J Biol Chem **277:** 24399–24404

Shimazaki KI, Sugahara K (1979) Specific inhibition of photosystem II activity in chloroplasts by fumigation of spinach leaves with SO_2. Plant Cell Physiol **20:** 947–955

Shimojima M (2011) Biosynthesis and functions of the plant sulfolipid. Prog Lipid Res **50:** 234–239

Sokolenko A, Pojidaeva E, Zinchenko V, Panichkin V, Glaser VM, Herrmann RG, Shestakov SV (2002) The gene complement for proteolysis in the cyanobacterium *Synechocystis* sp. PCC 6803 and *Arabidopsis thaliana* chloroplasts. Curr Genet **41:** 291–310

Stricks W, Kolthoff IM, Kapoor RC (1955) Equilibrium constants of the reaction between sulfite and oxidized glutathione. J Am Chem Soc **77:** 2057–2061

Takahashi H, Kopriva S, Giordano M, Saito K, Hell R (2011) Sulfur assimilation in photosynthetic organisms: molecular functions and regulations of transporters and assimilatory enzymes. Annu Rev Plant Biol **62:** 157–184

Tanaka K, Kondo N, Sugahara K (1982a) Accumulation of hydrogen peroxide in chloroplasts of SO_2-fumigated spinach leaves. Plant Cell Physiol **23:** 999–1007

Tanaka K, Otsubo T, Kondo N (1982b) Participation of hydrogen peroxide in the inactivation of Calvin-cycle SH enzymes in SO_2-fumigated spinach leaves. Plant Cell Physiol **23:** 1009–1018

Tsakraklides G, Martin M, Chalam R, Tarczynski MC, Schmidt A, Leustek T (2002) Sulfate reduction is increased in transgenic *Arabidopsis thaliana* expressing 5′-adenylylsulfate reductase from *Pseudomonas aeruginosa*. Plant J **32:** 879–889

Van Der Kooij TAW, De Kok LJ, Haneklaus S, Schnug E (1997) Uptake and metabolism of sulphur dioxide by *Arabidopsis thaliana*. New Phytol **135:** 101–107

Vauclare P, Kopriva S, Fell D, Suter M, Sticher L, von Ballmoos P, Krähenbühl U, den Camp RO, Brunold C (2002) Flux control of sulphate assimilation in *Arabidopsis thaliana*: adenosine 5′-phosphosulphate reductase is more susceptible than ATP sulphurylase to negative control by thiols. Plant J **31:** 729–740

Veeranjaneyulu K, N'soukpoé-Kossi CN, Leblanc RM (1991) SO_2 effect on photosynthetic activities of intact sugar maple leaves as detected by photoacoustic spectroscopy. Plant Physiol **97:** 50–54

Wang Y, Lin A, Loake GJ, Chu C (2013) H_2O_2-induced leaf cell death and the crosstalk of reactive nitric/oxygen species. J Integr Plant Biol **55:** 202–208

Watanabe M, Balazadeh S, Tohge T, Erban A, Giavalisco P, Kopka J, Mueller-Roeber B, Fernie AR, Hoefgen R (2013) Comprehensive dissection of spatiotemporal metabolic shifts in primary, secondary, and lipid metabolism during developmental senescence in Arabidopsis. Plant Physiol **162:** 1290–1310

Wu Y, Zheng F, Ma W, Han Z, Gu Q, Shen Y, Mi H (2011) Regulation of NAD(P)H dehydrogenase-dependent cyclic electron transport around PSI by $NaHSO_3$ at low concentrations in tobacco chloroplasts. Plant Cell Physiol **52:** 1734–1743

Yarmolinsky D, Brychkova G, Fluhr R, Sagi M (2013) Sulfite reductase protects plants against sulfite toxicity. Plant Physiol **161:** 725–743

Yesbergenova Z, Yang G, Oron E, Soffer D, Fluhr R, Sagi M (2005) The plant Mo-hydroxylases aldehyde oxidase and xanthine dehydrogenase have distinct reactive oxygen species signatures and are induced by drought and abscisic acid. Plant J **42:** 862–876

Yi H, Galant A, Ravilious GE, Preuss ML, Jez JM (2010) Sensing sulfur conditions: simple to complex protein regulatory mechanisms in plant thiol metabolism. Mol Plant **3:** 269–279

Yi X, McChargue M, Laborde S, Frankel LK, Bricker TM (2005) The manganese-stabilizing protein is required for photosystem II assembly/stability and photoautotrophy in higher plants. J Biol Chem **280:** 16170–16174

Yonekura-Sakakibara K, Onda Y, Ashikari T, Tanaka Y, Kusumi T, Hase T (2000) Analysis of reductant supply systems for ferredoxin-dependent sulfite reductase in photosynthetic and nonphotosynthetic organs of maize. Plant Physiol **122:** 887–894

Ziegler I, Libera W (1975) The enhancement of CO_2 fixation in isolated chloroplasts by low sulfite concentrations and by ascorbate. Z Naturforsch C **30:** 634–637